

NiO-doped $\text{CaCu}_3\text{Ti}_4\text{O}_{12}$ Thin Film by Sol-Gel Method

XU Dong^{1,2}, SONG Qi¹, ZHANG Ke¹, XU Hong-Xing¹, YANG Yong-Tao¹, YU Ren-Hong³

(1. School of Material Science and Engineering, Jiangsu University, Zhenjiang 212013, China; 2. State key Laboratory of Electronic Thin Films and Integrated Devices, University of Electronic Science and Technology of China, Chengdu 610054, China; 3 Changzhou Ming Errui Ceramics Co., Ltd., Changzhou 213102, China)

Abstract: Pure $\text{CaCu}_3\text{Ti}_4\text{O}_{12}$ (CCTO) thin film and NiO-doped $\text{CaCu}_{3-x}\text{Ni}_x\text{Ti}_4\text{O}_{12}$ (CCNTO) thin film with $x=0.10, 0.20$ and 0.30 were prepared by Sol-Gel method. The effects of NiO on the dielectric properties and microstructure revolution of CCTO were studied. The crystalline structure and the surface morphology of the films were markedly influenced by NiO content. AFM images of the $\text{CaCu}_{3-x}\text{Ni}_x\text{Ti}_4\text{O}_{12}$ samples showed that the grain size of Ni-doped CCTO was smaller than the grain size of CCTO without Ni doping. For the CCNTO thin film ($x=0.2$), the lowest leakage current was obtained and the minimum value reached 0.564 mA . Meanwhile, the highest threshold voltage and nonlinear coefficient were 81 V/mm and 1.9 , respectively. The dielectric constant increased when the doping content of Ni reached a certain level. Besides, the dielectric loss was decreased firstly, and then increased.

Key words: $\text{CaCu}_3\text{Ti}_4\text{O}_{12}$; Sol-Gel; electrical properties; microstructure

In recent years, as the electronic industry towards the direction of miniaturization, environmental protection, integration and low cost, the kind of perovskite structure of the $\text{CaCu}_3\text{Ti}_4\text{O}_{12}$ (CCTO) has become the focus of research because of its high dielectric constant, low dielectric loss, good thermal stability, low sintering temperature and excellent properties.

The huge dielectric constant of calcium copper titanate (CCTO) ceramic materials was discovered and reported by Subramanian in 2000^[1]. That CCTO had remarkably strong nonlinear current-voltage characteristics without dopant was demonstrated by Chung, *et al.*^[2] in 2004. Homes, *et al.*^[3] discovered that the relative dielectric constant, ϵ_r , of single crystalline $\text{CaCu}_3\text{Ti}_4\text{O}_{12}$ was close to 10^5 at frequencies below 20 kHz at 250 K . Furthermore, CCTO film materials were also found with very high dielectric constant. The CCTO is very sensitive to processing parameters which can affect its electrical properties such as dielectric constant. Extensive investigations have been made to identify the origin of the colossal dielectric property of CCTO^[4-8], whereas the nature and the origin of the giant dielectric constant of CCTO ceramics remain controversial. So far, researchers have put forward to all sorts of models to elucidate the phenomenon of the giant dielectric, such as mechanisms of polarization, Maxwell-Wagner relaxations. Among them, the internal barrier

layer capacitor (IBLC) effect which has been generally accepted as a well-founded explanation for the origin of the giant permittivity. Some studies have dealt with CCTO thin films grown by pulsed laser deposition (PLD), metal organic chemical vapor deposition, Sol-Gel and RF magnetron sputtering^[9-11]. Compared with the traditional methods, the Sol-Gel method has many advantages, such as simple process, no pollution, low energy consumption, and obtaining the higher degree (molecular scale) uniformity^[12-14]. Therefore, the Sol-Gel method was used in this study. Moreover, in the present form of CCTO materials, researches mainly focus on doping modification, and trying to further improve the dielectric properties. Doping is the common method in materials research.

The electrical properties can be greatly affected by appropriate doping and elements substitution. NiO is a kind of high dielectric material, however Ni-doped CCTO ceramics have not been reported previously. Therefore, we use the Sol-Gel method to prepare NiO-doped CCTO thin film, and investigate the influences of the Ni content on the microstructure and dielectric properties of CCTO.

1 Experimental procedure

Sol-Gel method was used to prepare the precursor of $\text{CaCu}_3\text{Ni}_x\text{Ti}_4\text{O}_{12+x}$, for $x=0, 0.1, 0.2, 0.3$ (samples labeled

Received date: 2013-03-04; **Modified date:** 2013-04-01; **Published online:** 2013-06-04

Foundation item: Specialized Research Fund for the Doctoral Program of Higher Education of China(20123227120021); Natural Science Foundation of Jiangsu Province(BK2012156); Universities Natural Science Research Project of Jiangsu Province (13KJB430006); Opening Project of State key Laboratory of Electronic Thin Films and Integrated Devices(KFJJ201105); Application Program for Basic Research of Changzhou(CJ20125001)

Biography: XU Dong, PhD, associate professor. E-mail: frankxud@126.com

CB0, CB1, CB2 and CB3, respectively). Reagent-grade raw materials were calcium acetate $[\text{Ca}(\text{CH}_3\text{COO})_2 \cdot \text{H}_2\text{O}]$, copper nitrate $[\text{Cu}(\text{NO}_3)_2 \cdot 3\text{H}_2\text{O}]$, $\text{Ni}(\text{NO}_3)_2$ and tetrabutyl titanate $[\text{Ti}(\text{OC}_4\text{H}_9)_4]$. Firstly, an appropriate amount of $\text{Ca}(\text{CH}_3\text{COO})_2 \cdot \text{H}_2\text{O}$, $\text{Cu}(\text{NO}_3)_2 \cdot 3\text{H}_2\text{O}$, $\text{Ni}(\text{NO}_3)_2$ and $\text{Ti}(\text{OC}_4\text{H}_9)_4$ in the stoichiometric ratio were dissolved in ethanol separately with some glacial acetic acid. Secondly, proper amount of deionized water and little amount nitric acid were added when the sol was stirred. After continual stirring for about 20 min, a cyan precursor sol was obtained. And then, the precursor sol aged for 30 h. Thirdly, CCTO thin films were deposited on Si substrate by dip-coating technique. Finally, CCTO thin film samples were annealed at 900°C for 1 h with a heating rate of $5^\circ\text{C}/\text{min}$.

For the characterization of electrical properties, the silver paste was coated on the face of samples, and the silver electrodes were formed by heating at 600°C for 10 min. The silver electrodes were 5 mm in diameter. The voltage-current (V - I) characteristics were measured using a V - I source/measure unit (CJP CJ1001). The nominal varistor voltages (V_N) at 0.1 and 1.0 mA were measured and the threshold voltage was at V_T (V/mm) ($V_T = V_N$ (1 mA)/ d ; d is the thickness of the sample in mm)^[15-17]. The leakage current (I_L) was measured at $0.75 V_N$ (1 mA). The measurement accuracy for voltage was $\pm 0.5\%$ and for electric current was $\pm 2\%$ ^[18-21]. In addition, the nonlinear coefficient

$\alpha(\alpha = 1/\lg(V_{1.0 \text{ mA}}/V_{0.1 \text{ mA}}))$ was determined with relative error of $\pm 5\%$ ^[22-24]. The crystalline phases were identified by X-ray diffraction (XRD, Rigaku D/max 2500, Japan) using a Cu K α radiation. The dielectric characteristics, such as the apparent dielectric constant (ϵ_r) and dissipation factor ($\tan\delta$) at different frequencies were measured by an HP4294A impedance analyzer (Agilent). The microstructures were evaluated by Atomic Force Microscope (SPM, SPA400, Seiko, Japan).

2 Results and discussion

Figure 1 shows the AFM images of Ni-doped CCTO films with different Ni contents. It is apparent that the grain size of CCTO without Ni doped is larger than that with Ni doped. The average grain size decreases gradually with the increase of Ni content. With the Ni content increase, the roughness of film surface firstly increases and then decreases when $x > 0.1$ (Table 1), which indicates that doping properly with NiO can further inhibit the growth of CCTO grains in the sintering process.

Table 1 Roughness characterization of the surface of Ni-doped CCTO films

Samples	CB0	CB1	CB2	CB3
Roughness, R_a/nm	65.1	141.3	76.1	10.7

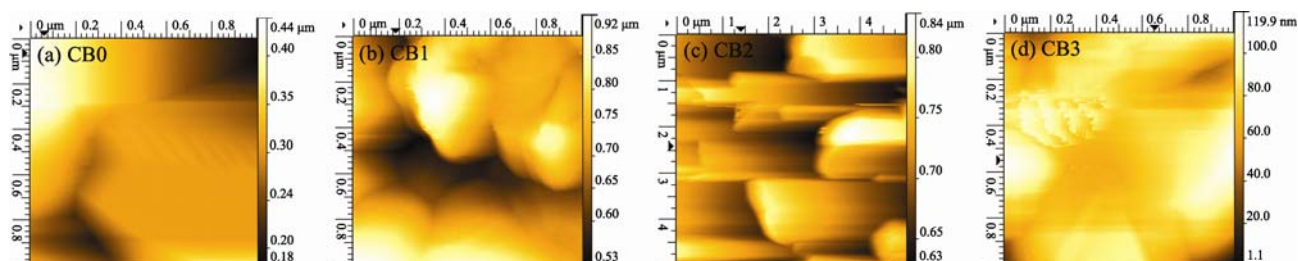


Fig. 1 AFM images of the surface of Ni-doped CCTO films

Figure 2 shows XRD patterns of the CCTO films with different dopant content. These patterns are essentially similar to that of undoped CCTO films. XRD data was indexed on the basis of a cubic unit cell which was similar to CCTO. The formation of $\text{CaCu}_3\text{Ti}_4\text{O}_{12}$ cubic phase belonging to the Im-3 space group (ICDD 75-2188) is apparent and reflections (220), (400) and (422) of $\text{CaCu}_3\text{Ti}_4\text{O}_{12}$ phase are identified for the Ni-doped CCTO films. In addition, the peaks of TiO_2 and CaTiO_3 indicate that there are TiO_2 phase in all samples. That tetrabutyl titanate is not pure probably leads to the existence of TiO_2 phase. The XRD peaks intensify with the increasing of Ni doping content, which suggest that dopant promotes the formation of the main crystalline phase of CCTO.

Figure 3 illustrates the dielectric constant and dielectric loss in frequency ranging from 1 kHz to 10 MHz at room temperature. The ϵ_r of the pure CCTO is about

26000 at 1 kHz. The dielectric constant decreases firstly and then increases with the increase of the Ni doping content. When $x=0.1$ and 0.2, the dielectric constant of NiO-doped CCTO is smaller than CCTO without NiO. When $x=0.3$, the dielectric constant of NiO-doped CCTO is much higher than

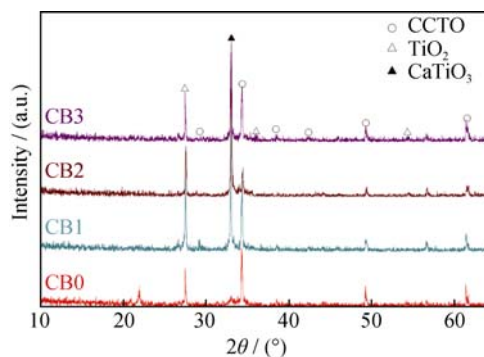


Fig. 2 XRD patterns of various Ni-doped CCTO film

others. Furthermore, the dielectric constant decreases with the frequency increases. According to the previous work^[7], the larger grain size will help to obtain a higher dielectric constant. In Fig. 3(b), the dielectric loss decreases firstly and then increases and the relaxation peak tends to move towards low frequency with the content of NiO increase. The dielectric loss in low frequency area is closely connected with leakage current of CCTO. The dielectric loss greatly increases with the content of NiO increase. Due to the addition of NiO, the carrier density in CCTO greatly increases, and the carrier in CCTO is electronic. Because Ni^{2+} replaces the position of Cu^{2+} , the content of CuO decreases, which leads to significant increase of the electronic concentration.

XPS analysis was carried out to investigate the valence states of ions in CCTO films. Figure 4 shows the XPS spectra of O1s, Ca2p, Ti2p, Cu2p and Ni2p. The shift of core-level spectra due to charging effect is calibrated using the contaminated C1s peak located at 285 eV. O1s peak of CBO without Ni doped can be spitted into two peaks from Figure 4(a). One is due to Cu–O bonds and the other is due to Ca–O bonds. Ni–O bonds are found in the O1s of CB1, CB2, CB3 with Ni doped. The XPS spectra of Ca2p, Ti2p, Cu2p and Ni2p are shown respectively in Figure 4 (b), (c), (d) and (e). It reveals that the presence of calcium in +2 oxidation state

is clear from the shape, the symmetry of the peak and the bonding energy of Ca2p in (b). The XPS patterns of Ti2p are shown in Figure 4 (c). It is clear that titanium is in the +4 state. The presence of titanium in +4 state is evident from the shape, the symmetry of the peak and the bonding energy of Ti2p. Small amounts of Cu^+ are found in the Cu2p. The presence of copper in +1 and +2 was clear from Figure 4 (d). Figure 4(e) shows the XPS spectra of Ni2p. It is revealed that the presence of nickel in +2 oxidation state is clear from the shape, the symmetry of the peak and the bonding energy of Ni2p in Figure 4 (e). And the graph of O1s in Figure 4 (a) presents that the nickel divalent combines with O ions to form the Ni–O bonds.

As can be seen from Table 2, Ni doping shows remarkable influences on the nonlinear current-voltage properties of CCTO samples. With increasing Ni content, the leakage current firstly increases and then decreases, while nonlinear coefficient and threshold voltage present an opposite tendency. When $x=0.2$, the lowest leakage current is obtained and the minimum value reaches to 0.564; meanwhile, the highest threshold voltage and nonlinear coefficient are 81 V/mm and 1.9, respectively. Sample CB2 displays good varistor properties which exhibits the lowest leakage current, and shows better nonlinear V - I characteristics than that of other samples. It can be accounted for that Ni doping increases CCTO grain boundary barrier, leads to nonlinear coefficient and threshold voltage rising up, and leakage current reduction. All things considered, the optimal varistor characteristic of the films was shown in the sample of $x=0.2$.

3 Conclusions

The $\text{CaCu}_{3-x}\text{Ni}_x\text{Ti}_4\text{O}_{12}$ ($x=0, 0.1, 0.2, 0.3$) thin films were prepared by Sol-Gel method and dip-coating technique. The crystalline structure and the surface morphology of the films were markedly influenced by various NiO content. From AFM observations, the grain size of CCTO with Ni doped was smaller than that without Ni doped. In general, it is found that the $\text{CaCu}_{2.8}\text{Ni}_{0.2}\text{Ti}_4\text{O}_{12}$ (the sample with $x=0.2$) has the best properties with the highest nonlinear coefficient and threshold field, which must be

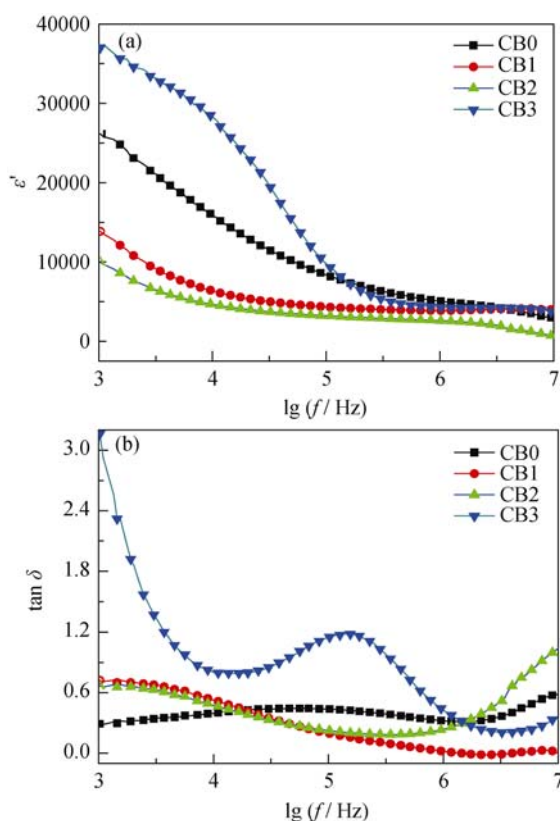


Fig. 3 Frequency dependence of (a) dielectric constant and (b) dielectric loss in Ni-doped CCTO films measured at room temperature

Table 2 Electrical properties of Ni-doped CCTO films

Sample	I_L/mA	V_T/mm	α
CB0	0.620	69	1.8
CB1	0.633	56	1.6
CB2	0.564	81	1.9
CB3	0.646	64	1.5

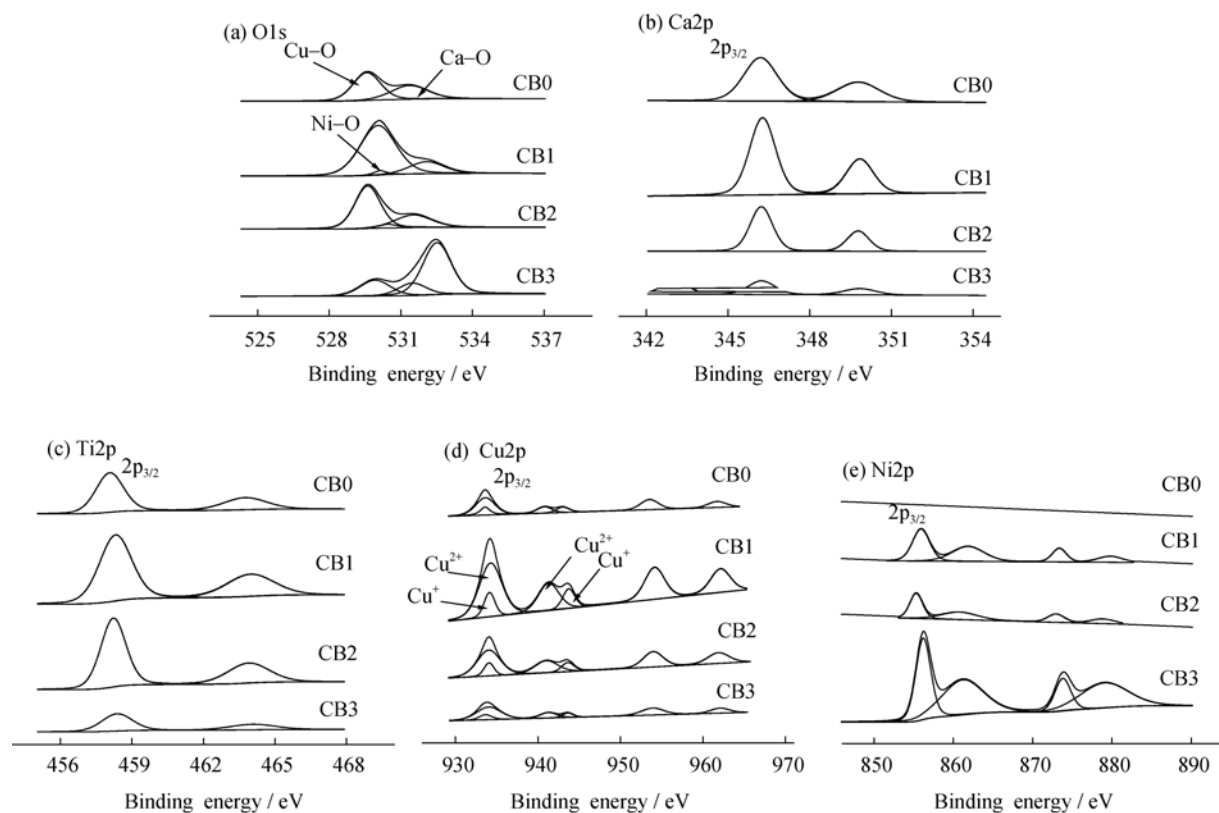


Fig. 4 XPS spectra of Ni-doped CCTO films
(a) O1s; (b) Ca2p; (c) Ti2p; (d) Cu2p; (e) Ni2p

accounted for that Ni doping increases CCTO grain boundary barrier, leading to nonlinear coefficient and threshold voltage rising up and leakage current reduction. The dielectric constant increases, when doping content reaches a certain level. The dielectric loss is decreased firstly and then increased. Owing to Ni does not reduce the dielectric loss, researchers can further reduce the loss to expect the promising application prospect of CCTO with NiO.

References:

- [1] Subramanian M A, Li D, Duan N, et al. High dielectric constant in $\text{ACu}_3\text{Ti}_4\text{O}_{12}$ and $\text{ACu}_3\text{Ti}_3\text{FeO}_{12}$ phases. *Journal of Solid State Chemistry*, 2000, **151(2)**: 323–325.
- [2] Chung S Y, Kim I D, Kang S. Strong nonlinear current-voltage behaviour in perovskite-derivative calcium copper titanate. *Nature Materials*, 2004, **3(11)**: 774–778.
- [3] Homes C C, Vogt T, Shapiro S M, et al. Optical response of high-dielectric-constant perovskite-related oxide. *Science*, 2001, **293(5530)**: 673–676.
- [4] Yuan W X, Hark S K. Investigation on the origin of the giant dielectric constant in $\text{CaCu}_3\text{Ti}_4\text{O}_{12}$ ceramics through analyzing $\text{CaCu}_3\text{Ti}_4\text{O}_{12}\text{-HfO}_2$ composites. *Journal of the European Ceramic Society*, 2012, **32(2)**: 465–470.
- [5] Xu D, Zhang C, Lin Y H, et al. Influence of zinc on electrical and microstructural properties of $\text{CaCu}_3\text{Ti}_4\text{O}_{12}$ ceramics prepared by Sol-Gel process. *Journal of Alloys and Compounds*, 2012, **522**: 157–161.
- [6] Xu D, Wang B, Lin Y H, et al. Influence of Lu_2O_3 on electrical and microstructural properties of $\text{CaCu}_3\text{Ti}_4\text{O}_{12}$ ceramics. *Physica B: Condensed Matter*, 2012, **407(13)**: 2385–2389.
- [7] Xu D, Zhang C, Cheng X N, et al. Dielectric properties of Zn-doped CCTO ceramics by Sol-Gel method. *Advanced Materials Research*, 2011, **197-198**: 302–305.
- [8] Li J Y, Xu T W, Li S T, et al. Structure and electrical response of $\text{CaCu}_3\text{Ti}_4\text{O}_{12}$ ceramics: effect of heat treatments at the high vacuum. *Journal of Alloys and Compounds*, 2010, **506(1)**: L1–L4.
- [9] Yuan W X, Hark S K, Xu H Y, et al. Investigation on the growth of $\text{CaCu}_3\text{Ti}_4\text{O}_{12}$ thin film and the origins of its dielectric relaxations. *Solid State Sciences*, 2012, **14(1)**: 35–39.
- [10] Bodeux R, Gervais M, Wolfman J, et al. $\text{CaCu}_3\text{Ti}_4\text{O}_{12}$ thin film capacitors: evidence of the presence of a Schottky type barrier at the bottom electrode. *Thin Solid Films*, 2012, **520(7)**: 2632–2638.
- [11] Deng G, Xanthopoulos N, Muralt P. Chemical nature of colossal dielectric constant of $\text{CaCu}_3\text{Ti}_4\text{O}_{12}$ thin film by pulsed laser deposition. *Applied Physics Letters*, 2008, **92(17)**: 172909–1–3.

- [12] Li Z, Fan H Q. Structure and electric properties of Sol-Gel derived $\text{CaCu}_3\text{Ti}_4\text{O}_{12}$ ceramics as a pyroelectric sensor. *Solid State Ionics*, 2011, **192(1)**: 682–687.
- [13] Parra R, Savu R, Ramajo L A, *et al.* Sol-Gel synthesis of mesoporous $\text{CaCu}_3\text{Ti}_4\text{O}_{12}$ thin films and their gas sensing response. *Journal of Solid State Chemistry*, 2010, **183(6)**: 1209–1214.
- [14] Zhang C H, Zhang K, Xu H X, *et al.* Microstructure and electrical properties of Sol-Gel derived Ni-doped $\text{CaCu}_3\text{Ti}_4\text{O}_{12}$ ceramics. *Transactions of Nonferrous Metals Society of China*, 2012, **22(s1)**: 127–132.
- [15] Xu D, Cheng X N, Wang M S, *et al.* Microstructure and electrical properties of La_2O_3 -doped $\text{ZnO-Bi}_2\text{O}_3$ -based varistor ceramics. *Advanced Materials Research*, 2009, **79-82**: 2007–2010.
- [16] Xu D, Shi L Y, Wu Z H, *et al.* Microstructure and electrical properties of $\text{ZnO-Bi}_2\text{O}_3$ -based varistor ceramics by different sintering processes. *Journal of the European Ceramic Society*, 2009, **29(9)**: 1789–1794.
- [17] Xu D, Cheng X N, Yan X H, *et al.* Sintering process as relevant parameter for Bi_2O_3 vaporization from $\text{ZnO-Bi}_2\text{O}_3$ -based varistor ceramics. *Transactions of Nonferrous Metals Society of China*, 2009, **19(6)**: 1526–1532.
- [18] Xu D, Cheng X N, Zhao G P, *et al.* Microstructure and electrical properties of Sc_2O_3 -doped $\text{ZnO-Bi}_2\text{O}_3$ -based varistor ceramics. *Ceramics International*, 2011, **37(3)**: 701–706.
- [19] Xu D, Cheng X N, Yuan H M, *et al.* Microstructure and electrical properties of $\text{Y}(\text{NO}_3)_3 \cdot 6\text{H}_2\text{O}$ -doped $\text{ZnO-Bi}_2\text{O}_3$ -based varistor ceramics. *Journal of Alloys and Compounds*, 2011, **509(38)**: 9312–9317.
- [20] Wu Z H, Fang J H, Xu D, *et al.* Effect of SiO_2 addition on the microstructure and electrical properties of ZnO -based varistors. *International Journal of Minerals, Metallurgy and Materials*, 2010, **17(1)**: 86–91.
- [21] Xu D, Shi X F, Cheng X N, *et al.* Microstructure and electrical properties of Lu_2O_3 -doped $\text{ZnO-Bi}_2\text{O}_3$ -based varistor ceramics. *Transactions of Nonferrous Metals Society of China*, 2010, **20(12)**: 2303–2308.
- [22] Xu D, Tang D M, Lin Y H, *et al.* Influence of Yb_2O_3 doping on microstructural and electrical properties of $\text{ZnO-Bi}_2\text{O}_3$ -based varistor ceramics. *Journal of Central South University*, 2012, **19(6)**: 1497–1502.
- [23] Xu D, Tang D M, Jiao L, *et al.* Comparative characteristics of yttrium oxide and yttrium nitric acid doping on ZnO varistor ceramics. *Journal of Central South University*, 2012, **19(8)**: 2094–2100.
- [24] Xu D, Tang D M, Jiao L, *et al.* Effects of high-energy ball milling oxide-doped and varistor ceramic powder on ZnO varistor. *Transactions of Nonferrous Metals Society of China*, 2012, **22(6)**: 1423–1431.

溶胶-凝胶法制备 NiO 掺杂 $\text{CaCu}_3\text{Ti}_4\text{O}_{12}$ 薄膜

徐 东^{1,2}, 宋 琪¹, 张 柯¹, 徐红星¹, 杨永涛¹, 于仁红³

(1. 江苏大学 材料科学与工程学院, 镇江 212013; 2. 电子科技大学 电子薄膜与集成器件国家重点实验室, 成都 610054; 3. 常州明尔瑞陶瓷有限公司, 常州 213102)

摘 要: 用溶胶-凝胶法制备纯 $\text{CaCu}_3\text{Ti}_4\text{O}_{12}$ (CCTO)薄膜以及 NiO 掺杂 $\text{CaCu}_{3-x}\text{Ni}_x\text{Ti}_4\text{O}_{12}$ (CCNTO)薄膜($x=0.10$ 、 0.20 、 0.30), 研究了掺杂 NiO 对 CCTO 介电性能以及微观结构的影响。通过 AFM 图片可以看出, 掺杂 NiO 的 CCTO 薄膜的晶粒尺寸比不掺杂 NiO 的 CCTO 薄膜的晶粒尺寸小。当 $x=0.2$ 时, CCNTO 薄膜的漏电流最小, 最小值为 0.546 mA , 同时具有最大阈值电压与最大非线性系数, 最大值分别为 81 V/mm 和 1.9 。当 Ni 掺杂量达到一定程度时, CCNTO 薄膜的介电常数就会增加, 总体来说, 随着 Ni 的掺杂量增加, CCNTO 薄膜的介电损耗呈上升趋势。

关 键 词: 钛酸铜钙; 溶胶-凝胶法; 电性能; 显微组织

中图分类号: TQ174

文献标识码: A